



# Performance and Energy Impact of Enhanced Cache Replacement Policy on STT-MRAM LLC

Pierre-Yves Péneau, David Novo, Florent Bruguier, Lionel Torres, Gilles Sassatelli, Abdoulaye Gamatié

## ► To cite this version:

Pierre-Yves Péneau, David Novo, Florent Bruguier, Lionel Torres, Gilles Sassatelli, et al.. Performance and Energy Impact of Enhanced Cache Replacement Policy on STT-MRAM LLC. 2021. lirmm-03341604

**HAL Id: lirmm-03341604**

**<https://hal-lirmm.ccsd.cnrs.fr/lirmm-03341604>**

Preprint submitted on 11 Sep 2021

**HAL** is a multi-disciplinary open access archive for the deposit and dissemination of scientific research documents, whether they are published or not. The documents may come from teaching and research institutions in France or abroad, or from public or private research centers.

L'archive ouverte pluridisciplinaire **HAL**, est destinée au dépôt et à la diffusion de documents scientifiques de niveau recherche, publiés ou non, émanant des établissements d'enseignement et de recherche français ou étrangers, des laboratoires publics ou privés.

# Performance and Energy Impact of Enhanced Cache Replacement Policy on STT-MRAM LLC

PIERRE-YVES PÉNEAU, DAVID NOVO, FLORENT BRUGUIER, LIONEL TORRES, GILLES SAS-SATELLI, and ABDOULAYE GAMATIÉ,

Laboratoire d'Informatique, de Robotique et de Microélectronique de Montpellier, France

Modern architectures adopt large on-chip cache memory hierarchies with more than two levels. While this improves performance, it has a certain cost in area and power consumption. In this paper, we consider an emerging non volatile memory technology, namely the Spin-Transfer Torque Magnetic RAM (STT-MRAM), with a powerful cache replacement policy in order to design an efficient STT-MRAM Last-Level Cache (LLC) in terms of performance and energy. Well-known benefits of STT-MRAM are their near-zero static power and high density compared to volatile memories. Nonetheless, their high write latency may be detrimental to system performance. In order to mitigate this issue, we combine STT-MRAM with a recent cache replacement policy. The benefit of this combination is evaluated through experiments on SPEC CPU2006 benchmark suite, showing performance improvements of up to 10% and 14% compared to SRAM cache with LRU respectively on single and multicore systems. Moreover, the energy consumption is on average decreased by 20% for all platforms.

Additional Key Words and Phrases: STT-MRAM, Last-Level Cache, Replacement Policy, Performance, Energy

## ACM Reference Format:

Pierre-Yves Péneau, David Novo, Florent Bruguier, Lionel Torres, Gilles Sassatelli, and Abdoulaye Gamatié. 2020. Performance and Energy Impact of Enhanced Cache Replacement Policy on STT-MRAM LLC. 1, 1 (September 2020), 23 pages.

## 1 INTRODUCTION

Energy consumption has become an important concern of computer architecture design for the last decades. While the demand for more computing resources is growing every year, much effort has been put on finding the best trade-off between performance and power consumption in order to build *energy-efficient* architectures. Current design trends show that the memory speed is not growing as fast as cores computing capacity, leading to the so-called *memory-wall* issue. Caching techniques, which have been pushed in the past for mitigating the memory-wall, are facing the silicon area constraints. As the memory hierarchy capacity is increased [45], the energy consumption of this part of the CPU scales accordingly. As an example, it constitutes up to 30% of the total energy of a StrongARM chip [28]. In particular, as the technology scaling continues, the static power consumption is becoming predominant over the dynamic power consumption [4].

---

Authors' address: Pierre-Yves Péneau, pierre-yves.peneau@lirmm.fr; David Novo, david.novo@lirmm.fr; Florent Bruguier, florent.bruguier@lirmm.fr; Lionel Torres, florent.bruguier@lirmm.fr; Gilles Sassatelli, florent.bruguier@lirmm.fr; Abdoulaye Gamatié, abdoulaye.gamatie@lirmm.fr, Laboratoire d'Informatique, de Robotique et de Microélectronique de Montpellier, 161 rue Ada, Montpellier, France, 34095.

---

Permission to make digital or hard copies of all or part of this work for personal or classroom use is granted without fee provided that copies are not made or distributed for profit or commercial advantage and that copies bear this notice and the full citation on the first page. Copyrights for components of this work owned by others than ACM must be honored. Abstracting with credit is permitted. To copy otherwise, or republish, to post on servers or to redistribute to lists, requires prior specific permission and/or a fee. Request permissions from [permissions@acm.org](mailto:permissions@acm.org).

© 2020 Association for Computing Machinery.

Data accesses that occur beyond the Last-Level Cache (LLC) are usually time and energy-consuming as they have to reach the off-chip main memory. An intelligent design of the LLC reducing such accesses can save power and increase the overall performance. A usual technique adopted in the past consists in increasing the cache storage capacity so as to reduce the cache miss rate. This approach is no longer desired due to area and energy constraints. Increasing the cache size has a negative impact on the financial cost and increases the static power consumption.

Here, we consider an emerging memory technology, the Spin-Torque Transfer Magnetic RAM (STT-MRAM), a Non-Volatile Memory (NVM) that has a near-zero leakage consumption. This memory has a higher density than SRAM, providing more storage capacity for the same area. While STT-MRAM read latency is close to SRAM read latency, the gap for write access is currently one obstacle to a wide STT-MRAM adoption.

The present work builds upon our previous studies [32, 34] and studies the impact in write reduction of cache replacement policies. Each read request leading to a cache miss eventually triggers a write. Upon this cache miss, the request is forwarded to an upper level in the memory hierarchy.<sup>1</sup> When the response is received, the corresponding data is written into the cache. Hence, the cache replacement policy has indirectly an important impact on the number of writes that occur upon cache misses. We carry out a fine-grained analysis on the actual sequence of read/write transactions taking place in the cache management strategy. This investigation focuses on performance and power consumption. On the basis of this study, we propose and evaluate the combined use of STT-MRAM and *state-of-the-art* Hawkeye cache replacement policy [18]. Thanks to Hawkeye, the number of writes due to cache misses is reduced, while benefiting from STT-MRAM density for larger LLC.

This paper is organized as follows: Section 2 presents related work; Section 3 introduces a motivational example and our writes analysis; Section 4 proposes a design space exploration for the Last-Level Cache with the STT-MRAM technology; Section 5 describes the experimental setup to validate our proposal; Section 6 discusses our experimental results; finally, Section 7 gives some concluding remarks and perspectives.

## 2 RELATED WORK

The use of hybrid caches has been a recurrent approach to address write asymmetry in NVMs. A hybrid cache mixes SRAM and NVM memories to achieve the best of each technology. Most existing techniques rely on a combination of hardware and software techniques.

Wu et al. [48] proposed a hybrid memory hierarchy based on a larger LLC thanks to NVM density. They evaluated different memory technologies and identified eDRAM as the best choice for performance improvement, while STT-MRAM is the best choice for energy saving. Sun et al. [43] designed a hybrid L2 cache with STT-MRAM and SRAM, and employed migration based policy to mitigate the latency drawbacks of STT-MRAM. The idea is to keep as many write intensive data in the SRAM part as possible.

Kim et al. [20] promoted the design of exclusive last-level cache using STT-RAM. In such a cache hierarchy, evicted blocks from lower-level cache are copied in the last-level cache regardless. The authors showed that their solution drastically reduces energy consumption of the last-level cache while enhancing the system performance.

Priya et al. [37] introduced a mechanism for improving the lifetime of STT-RAM. They leveraged the MRU (Most Recently Used) replacement algorithm to achieve their goal. They claimed an improvement of 4x compared to the mainstream LRU replacement algorithm.

<sup>1</sup>The first cache level (L1), the closest to the CPU, is the lowest level.

Senni et al. [39–41] proposed a hybrid cache design where the cache tag uses SRAM while cache data array uses STT-MRAM. The cache reacts at the speed of SRAM for hits and misses, which slightly mitigate the overall latency, while power is saved on the data array thanks to low leakage. Migration techniques for hybrid memories are expensive and may suffer from inaccurate predictions, inducing extra write operations.

Luo et al. [26], authors present a thrashing aware placement and migration policy (TAP) that address the thrashing blocks generation issue between L2 and LLC. They show how an adequate dirty thrashing blocks management in a hybrid memory architecture (combining SRAM and STT-MRAM) favors energy reduction while minimizing the performance loss.

Zhou et al. [50] proposed another technique called early-write-termination: upon a write, if the value to write is already in the cell, i.e., a redundant write [7, 8, 36], the operation is canceled. This technique, implemented at circuit level, does not require an extra read before writing and saves dynamic writing energy. Nevertheless, it is mainly relevant to applications with many redundant writes.

Software techniques to mitigate NVMs drawbacks have been also proposed. Li et al. [22] proposed a compilation method called migration-aware code motion. The goal is to change the data access patterns in cache blocks so as to minimize the extra cost due to migrations. Instructions that access the same cache block with the same operation are scheduled by the CPU close to each other. Péneau et al. [33] proposed to integrate STT-MRAM-based cache at L1 and L2 level and to apply aggressive code optimizations to reduce the number of writes. Albeit software approaches are portable to different architectures, they break the abstraction layer between hardware and software. Indeed, compiler has to know the underlying technology.

Smullen et al. [42] redesigned the STT-MRAM memory cells to reduce the high dynamic energy and write latency. They decreased the data retention time (i.e., the non-volatility period) and reduce the current required for writing. While this approach shows promising results, it relies on an aggressive retention reduction that incurs the introduction of a costly refresh policy to avoid data loss. Later on, Bouziane et al. [9] leveraged the data retention time tradeoff to show how to efficiently map data on NVM.

In this work, we take a complementary approach and evaluate the impact of cache replacement policies coupled with variations on LLC capacity in the reduction of critical writes. We basically re-evaluate the gap in performance between STT-MRAM and SRAM-based LLC given the latest advances in cache replacement policies. Moreover, energy results are also provided. We assess these changes on the entire memory hierarchy, while some previous work [22–25, 30, 43, 47, 49, 50] often use a partial perspective, i.e., a cache-level only.

### 3 MOTIVATION AND APPROACH

In this work, we use the ChampSim [1] simulator with a subset of applications from the SPEC CPU2006 benchmark suite [17] for motivating our approach. Compared to usual simulation tools used for evaluating NVM in system architectures, e.g. gem5 [6, 11, 13, 14] and SimpleScalar [10, 44], ChampSim is a faster simulator, yet less precise tool compared to gem5. It executes application traces instead of full codes. Note that trace-driven simulation is also possible with gem5 [12, 31]. Another benefit is that it can be easily customized to evaluate various cache replacement techniques, while it would be more tedious with an environment such as gem5. Timing and energy results are obtained from NVSim [15] for the LLC and from datasheet information for the main memory [2]. More details of the experimental setup are given in Section 5.1. A common metric used to assess LLC performance is the *Miss Per Kilo Instructions* (MPKI), defined as the total number of cache misses divided by the total number of executed instructions. One possibility to

reduce the MPKI is to increase the cache size. The cache contains more data and reduces the probability for a cache miss to occur. This results in penalties in terms of cache latency, energy and area.

### 3.1 Motivational Example

Let us evaluate the execution of two SPEC CPU2006 applications, namely *soplex* and *libquantum*. These applications have different memory access patterns. Figure 1a depicts the impact of 4MB versus 2MB LLC cache designs on the MPKI, the Instruction Per Cycle (IPC) and the energy consumption of LLC and the main memory. For *soplex*, the MPKI is decreased by 27.6%, leading to a faster execution by 9.7%, while the energy consumption of the LLC and the main memory is respectively damaged by 33% and improved by 23%. While the performance for *soplex* application benefits from a larger cache, this induces a negative impact on the LLC energy consumption. On the other hand, the outcome is different for the *libquantum* application. As shown in Figure 1a, the MPKI is unchanged (i.e., no improvement), while the IPC is slightly decreased by 0.6%. The energy consumption of the LLC and the main memory is also degraded, due to more expensive read/write transactions on the LLC. Moreover, a lower IPC, i.e., a longer execution time, increases the static energy. Here, the energy consumption of the LLC drastically grows by up to 47% with larger cache. The breakdown in static and dynamic energy consumption of the LLC is detailed in Figure 1b: 80% of the energy comes from the static part.

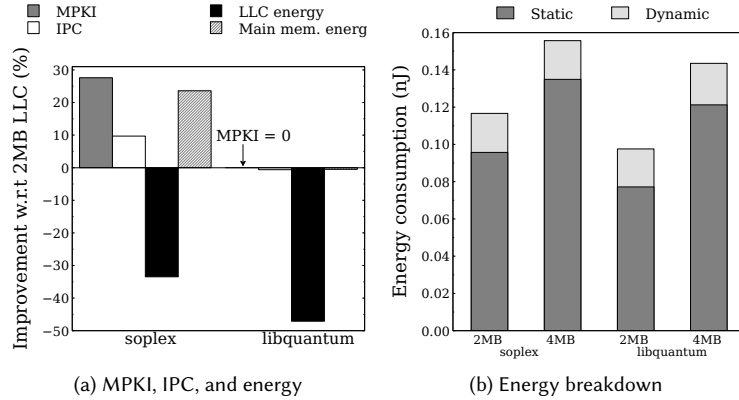


Fig. 1. Evaluation of 2MB and 4MB LLC for *soplex* and *libquantum*

Increasing the cache size shows interesting results for performance but faces two obstacles. Firstly, the LLC energy consumption is increased. Moreover, depending of the memory access pattern of the application, it may degrade the LLC energy while offering no gain in performance. Secondly, doubling the LLC size increases the silicon area on the chip. Nowadays, this aspect is crucial in design and larger caches are often not realistic due to area budget constraints. To tackle these two aspects, we consider STT-MRAM, which is considered as a future candidate for SRAM replacement [46]. The STT-MRAM technology suffers from higher memory access latency and energy per access than SRAM, especially for write operation. However, STT-MRAM memory cells are composed of one transistor, while it is six transistors for SRAM cells. Hence, STT-MRAM is a denser. In addition, this technology offers a near-zero leakage power, which eliminates the high static energy consumption observed with SRAM (see Figure 1b). This aspect is particularly relevant for applications that do not benefit from larger cache such as *libquantum* (see Figure 1b) In such a case, even though the

execution time is longer, the energy consumption would not dramatically increase thanks to the low static energy of STT-MRAM.

### 3.2 Writes Operations at Last-Level Cache

At Last-Level Cache, write operations are divided into two categories: *a) write-back*, i.e., a write operation coming from a lower cache level, and *b) write-fill*, i.e., a write operation that occurs when the LLC receives an answer from the main memory. These schemes are illustrated in Figure 2. Let us consider L3 cache as LLC. Transaction (1) is a *write-back* coming from the L2 for data  $X$ . In this case,  $X$  is immediately written in the cache line (transaction (2a)). Possibly, a *write-back* could be generated by the LLC towards the main memory (transaction (2b)) if data  $D$  has been modified and needs to be saved. For requests (3) and (4), corresponding respectively to a *read* and a *prefetch*, the requested  $Y$  data is not in the cache. This cache miss triggers a transaction to the main memory to fetch  $Y$ , and upon receiving the response,  $Y$  data is written in the cache. This operation represents a *write-fill*. As with transaction (2b), a *write-back* is generated if data  $L$  replaced in the LLC must be saved.

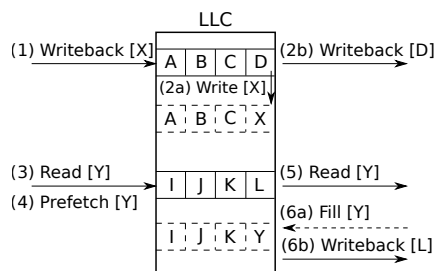


Fig. 2. Write transactions on the Last-Level Cache

Then, an important question that arises is to know whether or not *write-back* and *write-fill* have an equivalent impact on the overall system performance? For illustration, we consider five SPEC CPU2006 applications with different writes distributions to answer this question. Figure 3a reports the normalized IPC for different write latencies, while Figure 3b depicts the write distribution for the considered applications. Here,  $WF$  and  $WB$  respectively denote *write-fill* latency and *write-back* latency. We define the reference configuration as a 2MB STT-MRAM LLC with  $WF = WB = 38$  cycles. Results are normalized to this reference. We also compare with a 2MB SRAM LLC where  $WF = WB = 20$  cycles.

First, we set  $WF = 0$  cycle in order to assess the impact of the *write-fill* operation on system performance. Then, we apply the same for  $WB$  for evaluating the impact of *write-back*. We also compare to the specific configuration where both  $WF$  and  $WB$  are set to zero. For all configurations, the write-buffer contains up to 16 elements. Moreover, bypassing is disabled for *write-back*.

When  $WF = 0$  cycle, i.e., *write-fill* has no impact on performance, results show a reduced execution time by  $0.93\times$  on average and up to  $0.84\times$  for *libquantum*. When  $WB = 0$  cycle, i.e., *write-back* has no impact on performance, the execution time is the same as for the reference STT-MRAM configuration. Finally, when both  $WF$  and  $WB$  are set to zero, the execution time is the same as the case where only *write-fill* latency is set to zero. Performance gains are particularly visible for applications that have a higher number of *write-fill* than *write-back* requests, such as *libquantum* or *sphinx3*. Nevertheless, even for an application with more *write-back* requests such as *perlbench* (see Figure 3b), results show that  $WB = 0$  cycle has no impact on performance. These results show that only *write-fill* have a high impact on

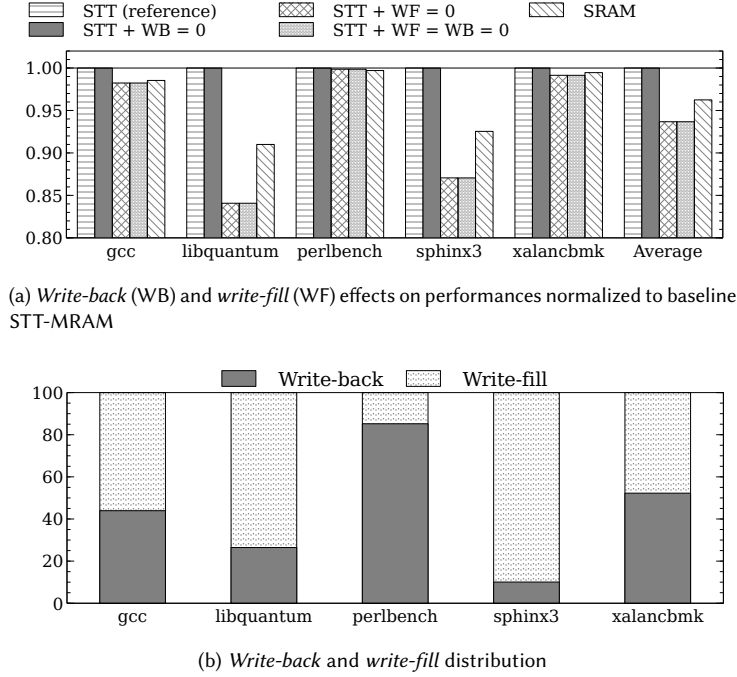


Fig. 3. Write operations performance and distribution

performance. Indeed, a *write-back* operation coming from a lower level of the memory does not require an immediate response from the LLC. Hence, it does not stall the CPU. Conversely, a *write-fill* occurs upon a cache miss, meaning that the CPU needs a data to continue the execution of an application. Unless the data becomes available, the CPU could be stalled if further instructions depend on this data.

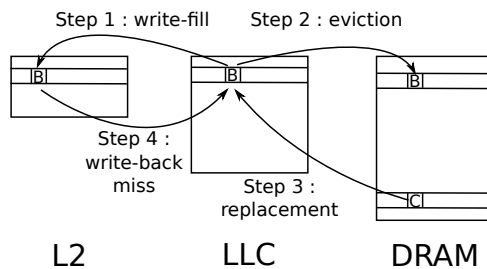
The above analysis shows that, with STT-MRAM, one should primarily focus on *write-fill* operations for reducing the number of writes on the LLC and improving system performance.

Moreover, our results show that there is no side-effect between these two types of write. Let us define  $A$  the performance improvement with  $WF = 0$ ,  $B$  the performance improvement with  $WB = 0$  and  $C$  the performance improvement with  $WF = WB = 0$ . Figure 3a shows that  $A + B = C$  for all applications. Hence,  $A$  does not have an impact on  $B$  and vice versa. Therefore, one could reduce the number of *write-fill* without a side effect on *write-back* in terms of performance.

### 3.3 Effects of write-fill reduction on the energy consumption

While a *write-fill* reduction has a positive effect in terms of performance, it could modify the type of requests on the LLC and by corollary the energy consumption. In this section, we examine what are these changes and their impact. Then, we analyze these effects on SRAM and STT-MRAM technologies.

**3.3.1 Changes on memory accesses.** Let us consider a memory hierarchy with inclusive L1 and L2 caches and an exclusive LLC. With such an architecture, the eviction of a block in the LLC does not evict this block in other caches.

Fig. 4. Illustration of the *write-back miss* effect

The reduction of *write-fill* means that read requests from the L2 have to priority over the write requests. Whenever a block  $B$  is detected in the LLC as useless for reading, it is discarded and replaced. However, block  $B$  could be written in the future in the LLC if the L2 generates a *write-back* request for  $B$ . This scheme is described on the Figure 4. First,  $B$  is sent from the LLC to the L2 (step 1). Then, the LLC evicts  $B$  which is replaced by  $C$  (step 2 and 3). When the L2 generates a *write-back* request for  $B$ , the block is missing and it generates a *write-back miss*.  $C$  is evicted, and  $B$  is written. If  $B$  had not been evicted, the *write-back* would have generate a *hit*. Note that in both cases, the latency remains the same. This slight difference between *write-back hit* and *write-back miss* is not perceptible in terms of performance, but the energy requirement is different.

Equations 1 and 2 reflect the dynamic energy consumption of the LLC:

$$E_{rd} = P_r^h \times E_r + \{(1 - P_r^h) \times (E_r + E_m)\} \quad (1)$$

$$E_{wr} = P_w^h \times E_w + \{(1 - P_w^h) \times (E_w + E_m)\} , \quad (2)$$

where  $E_{rd}$  and  $E_{wr}$  respectively denote the total dynamic energy consumption for reading and writing,  $E_r$ ,  $E_w$  and  $E_m$  the energy consumption for a single read, write or miss, and  $P_r^h$  and  $P_w^h$  the probability of *read hit* and *write-back hit*. Decreasing the number of *write-fill* means increasing  $P_r^h$ . Hence, reading becomes less costly since one avoid the cost of a miss,  $E_m$ . As previously mentioned, a side-effect of this choice could be to reduce  $P_w^h$ . In such a case, writing becomes more costly since a miss has been added. In a *write-fill*-optimized scenario where  $P_r^h$  is increased and  $P_w^h$  is decreased, the dynamic energy consumption of the LLC could be greater than a scenario without *write-fill* optimization.

**3.3.2 Difference between SRAM and STT-MRAM.** Changes on the dynamic energy consumption of the LLC do not have the same effect according to the technology used for the cache. Equation 3 depicts the energy consumption of the LLC, regardless of the technology:

$$E = \alpha(W \times T) + \beta(E_{rd} + E_{wr}) , \quad (3)$$

where  $W$  is the static power of the LLC,  $T$  the execution time, and  $\alpha$  and  $\beta$  two variables.  $\alpha(W \times T)$  and  $\beta(E_{rd} + E_{wr})$  respectively denote the static part and the dynamic part of the energy consumption. A cache that uses SRAM technology has a total energy consumption mostly dominated by the static part, i.e.,  $\alpha \gg \beta$ . An aggressive optimization on *write-fill* would decrease the total execution time  $T$ , and by corollary the static energy consumption. However, even if the dynamic power is increased, the relation  $\alpha \gg \beta$  remains true. Then, the overall energy consumption of the LLC is decreased.

This behavior is not observable with the STT-MRAM technology. One key property of STT-MRAM is its very low static power. Then, the relation between  $\alpha$  and  $\beta$  is reversed and  $\alpha \ll \beta$ . In such a case, an increase of the dynamic energy

consumption is not masked by the static part as with the SRAM technology. Then, a cache that uses the STT-MRAM technology could suffer from a greater energy consumption when using optimization on *write-fill* than without.

### 3.4 Cache Replacement Policy

*Write-fill* operations are directly dependent on the MPKI of the LLC. A low MPKI leads to a low amount of requests to the main memory, and then a low amount of *write-fill* operations. Thus, one way to mitigate the STT-MRAM write latency is to reduce the MPKI to decrease the number of *write-fill* requests.

The cache replacement policy is responsible for data eviction when a cache line is full. For example, in Figure 2, data  $X$  of the *write-back* transaction erases data  $D$ . It means that  $D$  has been chosen by the replacement policy to be evicted. Hence, the next access to  $D$  will generate a cache miss. Therefore, the replacement policy directly affects the number of misses, and so the MPKI. An efficient policy should evict data that will not be re-used in the future, or at least be re-used further than the other data in the same cache line. The most common used policy is the Least-Recently Used (LRU), which is cheap in terms of hardware resources. However, it is well-known that LRU is not the most efficient policy [38] and is also far from the theoretical optimal that could be achieved [16]. The *state-of-the-art* Hawkeye [18] replacement policy has been developed as an attempt to bridge this gap. This policy is based on the theoretical MIN algorithm, *a.k.a.* Belady’s algorithm [5]. To the best of our knowledge, this is the most advanced replacement policy [3].

This strategy identifies instructions that often generate cache misses. For a certain number of cache accesses, a data structure called a *predictor* keeps in memory the result of each access, *i.e.*, *hit* or *miss*, by using saturating counters. The program counter of the instruction that has generated the access is also saved. Hence, the memory of the predictor contains instructions that generate *hits* or *misses*. Upon each cache access, the predictor is consulted, a prediction is made and saturating counters are updated. Cache blocks, which are accessed by instructions generating cache misses have higher priority for eviction.

## 4 NON-VOLATILE MEMORY EXPLORATION

### 4.1 Leveraging the density of STT-MRAM

Large LLC memory capacity allows to store more data and avoid costly accesses to the main memory.<sup>2</sup> As a result, LLC accesses become more expensive in terms of latency and energy, while the leakage power increases as the area is doubled.

For the same cache capacity, STT-MRAM requires a smaller silicon area footprint than SRAM thanks to its higher density. In other words, STT-MRAM provides larger cache memory capacity for the same silicon area. In this work, we exploit this feature, to enlarge the LLC capacity up to the silicon area of the reference SRAM LLC. Hence, the following constraint must be satisfied:

$$A_{sram} \geq A_{stt}, \quad (4)$$

where  $A_{sram}$  is the silicon area of the reference LLC in SRAM and  $A_{stt}$  is the silicon area of the LLC in STT-MRAM. The reference LLC selected in our study is a SRAM cache with a storage capacity of 2MB for monocore systems and 4MB for multicore systems. We use NVSim [15] to determine that the STT-MRAM LLC size can be increased up to 8MB and 16MB within the reference cache area constraint respectively for monocore and multicore systems (see more details in Section 5). Each cache size above this limit breaks the constraint expressed by Formula 4.

<sup>2</sup>Note that some applications may not benefit from this feature. When memory accesses have no spatial locality, the cache architecture cannot capture this behavior and all accesses would eventually miss, regardless of the cache size.

Criterion	Description
ADP	MIN(Area-Delay Product)
AD <sup>2</sup> P	MIN(Area-Delay-Square Product)
ADEP	MIN(Area-Delay-Energy Product)
ADE <sup>2</sup> P	MIN(Area-Delay-Energy-Square Product)
ReadEDP	MIN(ReadDelay*ReadEnergy)
WriteEDP	MIN(WriteDelay*WriteEnergy)

Table 1. Selection criteria for cache memory configurations

## 4.2 Design exploration with NVSim

Usually, authors use NVSim to extract a cache configuration and give no explanation on how do they obtain these results. In this paper, we propose an extensive NVM exploration in order to select the best cache configuration according to a given criterion. To the best of our knowledge, this kind of design space exploration has never been presented in a paper.

*4.2.1 Methodology.* Our exploration is conducted with NVSim and adopt the following method :

- A minimal definition of the cache configuration
- An automatized exploration based on this definition
- The definition of a criterion to select a configuration
- A visualization of the exploration space
- The application of our criterion to select an appropriate configuration

We set five parameters in the minimal definition of a cache: memory size, word size, associativity, technology and temperature. The automatized process of exploration relies on the exploration mode provided by NVsim. For all parameters without a pre-defined value, NVSim explores a large variety of possibilities and store all results in a CSV file.

*4.2.2 Criterion selection.* There is different criteria of design selection based for example on the latency or the energy costs. Each of these criterion is usually used according to the considered cache level. For instance, a first-level cache should treat CPU requests in a fast manner. Hence, the latency criterion is pre-dominant over the energy. On the contrary, a Last-Level Cache should be optimized for its static energy, which is correlated to its area. Table 1 summarizes six criteria we identified for a cache configuration selection.

Since STT-MRAM is known for its high delay and energy, we want to reduce these values as much as possible. Moreover, we set an area constraint on the LLC for our exploration (see Formula 4). Then, we choose to take into account the area in our choice and select the Area-Delay-Energy Product (ADEP) as our main discriminant. This is a balanced choice between all three parameters that we need.

*4.2.3 Result visualization.* Figure 5 shows the design space exploration for a 4MB 16-way cache. There is a total of 72192 possible designs. For the sake of visibility, we perform a zoom on the most interesting region of the plot. Each point denotes an energy value. The intersection of this value, the area value and the delay value gives one possible design. Black points are the Pareto design according to these three metrics. The point surrounded with a square is the selected ADEP design. We repeat this process for all STT-MRAM cache configuration used in this paper. Results are summarized in Table 2.

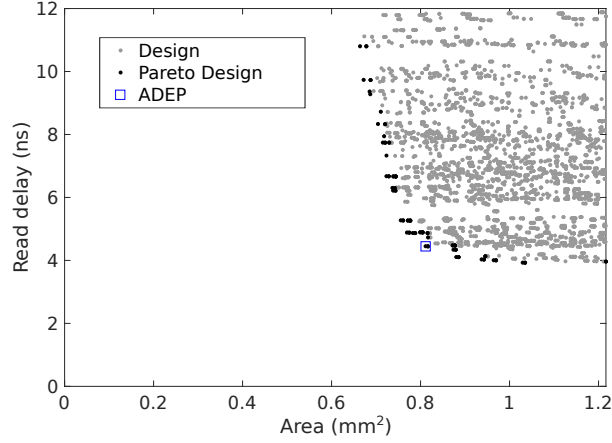


Fig. 5. Pareto view of all cache configurations for read delay according to cache area

## 5 EXPERIMENTAL SETUP

### 5.1 Environment Setup

We describe the timing, area and power models used in the sequel for the LLC and the main memory. Then, we introduce the used simulation infrastructure and we explain its calibration with considered timing information.

**5.1.1 Memory Model.** For both LLC models, we used  $22\text{ nm}$  technology with a temperature of  $350\text{ K}$ . The considered STT-MRAM model is provided with NVSim and assumes optimization for cell area, set/reset pulse duration and energy. The obtained parameter values are summarized in Table 2 and are compliant with state-of-the-art projection for this technology scaling [29].

The considered main memory model is based on a publicly available datasheet from Micron Technology [2]. We modeled a 4GB DDR3 with 1 DIMM, 8 ranks, 8 banks per ranks, organized with  $16 \times 65536$  columns with 64B on each row. Thus, each bank contains 64MB of data, each rank 512MB, and the total is 4GB. The extracted latency parameters are given in Table 3. For multicore systems with 8GB of memory, we add another DIMM with the same characteristics.

**5.1.2 Power models. Caches memory.** For each cache level, we extract the energy cost of each memory operation, i.e., read, write and miss, and multiply it by the number of reads, writes and misses observed on this cache level, as follows:

$$E^i = \{R^i \times E_R^i + W^i \times E_W^i + M^i \times E_M^i\} + \{T \times P_{leak}^i\}, \quad (5)$$

where  $i$  is the  $i^{th}$  cache level;  $R^i$ ,  $W^i$  and  $M^i$  are respectively the numbers of reads, writes and misses;  $E_R^i$ ,  $E_W^i$  and  $E_M^i$  are respectively the costs of a read, a write and a miss operation;  $T$  is the execution time and  $P_{leak}^i$  is the leakage power. The first part between braces represents the dynamic energy consumption and the second part the static energy consumption.

**Main memory.** In addition to the latency model, Table 3 contains information extracted from the Micron datasheet [2] to create a power model for the main memory. Here,  $RD$  and  $WR$  are respectively the unit cost per read and write;  $PRE$

Table 2. SRAM and STT-MRAM timing and area results configurations.

	SRAM				STT-MRAM			
	2MB	4MB	8MB	16MB	2MB	4MB	8MB	16MB
Read latency [ns]	1.43	2.10	3.74	6.53	4.43	4.45	5.05	5.55
Write latency [ns]	-				6.00	6.05	6.31	6.52
Read energy [nJ]	0.07	0.10	0.14	0.19	0.20	0.25	0.26	0.29
Write energy [nJ]	0.06	0.09	0.13	0.18	0.25	0.30	0.30	0.33
Miss energy [nJ]	0.001	0.002	0.003	0.004	0.12	0.12	0.12	0.12
Static power [mW]	30.40	62.17	124.25	233.10	1.85	4.44	8.98	16.72
Area [mm <sup>2</sup> ]	1.52	3.02	5.78	11.21	0.45	0.81	1.54	2.99

Table 3. Main memory configuration parameters [2]

$t_{RP}$	$t_{RCD}$	$t_{CAS}$	$t_{RAS}$	$t_{RFC}$	$t_{CK}$
11 cycles			28 cycles	208 cycles	1.25ns

$RD$	$WR$	$PRE$	$ACT$	$ACT_{BG}$	$REF$	$T_{REF}$
0.47nJ	0.47nJ	0.22nJ	0.38nJ	0.027W	46.33nJ	64ms

and  $ACT$  are respectively the cost of page pre-charge and page activation;  $ACT_{BG}$  is the active background energy consumption;  $REF$  is the cost of a refresh and  $T_{REF}$  is the self-refresh frequency of the main memory.

We use the following formula [27] to compute the energy consumption of the main memory:

$$E_m = E_a + E_b + E_c, \quad (6)$$

$$E_a = R \times RD + W \times WR, \quad (7)$$

$$E_b = (R_M + W_M) \times (PRE + ACT), \quad (8)$$

$$E_c = (T/T_{REF}) \times REF + T \times ACT_{BG}, \quad (9)$$

where  $E_m$  is the total energy consumption of the main memory,  $E_a$  the energy consumption due to read and write,  $E_b$  the energy consumption due to row buffer miss which triggers pre-activation and activation of memory pages, and  $E_c$  is the static energy consumption due to page refresh and static power.<sup>3</sup> For Equation 7,  $R$  and  $W$  are the number of read and write. For Equation 8,  $R_M$  and  $W_M$  are the number of read miss and write miss. For Equation 9,  $T$  is the execution time.

**5.1.3 Simulation Environment.** Our evaluation is conducted with the ChampSim simulator [1] used for the Cache Replacement Championship at ISCA'17 conference [3]. The modeled architecture is based on an Intel Core i7 system. Cores are Out-of-Order with a 3-level on chip cache hierarchy plus a main memory. For multicore systems, we set the number of cores to 4. L1 and L2 caches are private to each core and the LLC is shared between all cores. The setup is specified in Table 4.

<sup>3</sup>There is no low-power mode in our model that could reduce  $ACT_{BG}$ .

Table 4. Experimental setup configuration.

L1 (I/D)	32KB, 8-way, LRU, Private, 4 cycles			
L2	256KB, 8-way, LRU, Unified, 8 cycles			
L3	Varying size/policy, 16-way, Shared			
L3 size	2MB	4MB	8MB	16MB
L3 SRAM latency	20	23	30	41
L3 STT latency (R/W)	33/39	33/39	35/40	37/41
Hawkeye budget	28.2KB	58.7KB	114.7KB	266.4
CPU	1 or 4 core(s), Out-of-Order, 4GHz			
Main mem. size/latency	4GB or 8GB, hit: 55 cycles, miss: 165 cycles			

Each trace represents an isolated region of interest of 1 billion instructions. Each core executes a single-threaded application during 1 billion instructions. The cache warm-up takes 200 millions instructions while the remaining 800 millions instructions are used to report execution statistics. For multicore platforms, we consider 20 mixes composed each by four SPEC CPU2006 applications. Mixes have been generated randomly from the 20 applications and are presented in Table 5. When a core finishes its 1 billion instructions, it continues to read the trace to simulate an activity on the memory hierarchy until all cores reach 1 billion of executed instructions. The extra activity related to this mechanism is not reported in the final results. We calculate the average performance, i.e., IPC, by applying a geometric mean on the IPCs measured for all applications, as previous work did [18, 19, 35].

Sixteen configurations are addressed in this study: 2MB LLC cache with SRAM and STT-MRAM; 4MB and 8MB LLC caches only with STT-MRAM; and each of these four caches is combined with either LRU or Hawkeye. This is the same setup for multicore platform except that it is shifted from 4MB to 16MB. For the sake of simplicity, we associate the prefixes T (for Tiny), S (for Small), M (for Medium) and B (for Big) together with technology names in order to denote respectively the 2MB, 4MB, 8MB and 16MB LLC configurations. The name of considered replacement policies, i.e., LRU and Hawkeye, are used as a suffix. For instance,  $T\_stt\_hwk$  denotes a 2MB STT cache, using the Hawkeye policy.

**5.1.4 Latency Calibration.** The total access time of LLC in SRAM is usually dominated by the transfer delay of the interconnect, and not by the cache access itself [21]. This mitigates the impact of the potential performance penalty resulting from the integration of STT-MRAM in LLC. Therefore, we define the total access time  $L_T$  for the LLC as follows:

$$L_T = L_C + L_I \quad (10)$$

where  $L_I$  is the interconnect latency and  $L_C$  the cache latency (see also Figure 6). Thus, the effective latency is the sum of the interconnect latency and the cache latency. Our evaluation framework is calibrated based on an Intel-i7 processor where the LLC latency for a 2MB SRAM cache is  $5ns$ , i.e.,  $L_T = 5ns$ . With NVSim, we extract the cache access latency of a 2MB SRAM cache and we obtained  $L_C = 1.34ns$ . Hence, we calculate the interconnect latency:

$$L_I = L_T - L_C = 3.66ns. \quad (11)$$

We set  $L_I$  to this value and use it as an offset to calculate the total access time for each cache configuration mentioned in Table 2. Then, we convert this latency in cycles w.r.t. the CPU frequency

Table 5. Detail of the 20 mixes executed on multicore platforms

	Core 0	Core 1	Core 2	Core 3
mix1	gobmk	libquantum	perlbench	xalancbmk
mix2	astar	bwaves	lbm	zeusmp
mix3	cactusADM	lbm	milc	perlbench
mix4	bwaves	lbm	sphinx3	wrf
mix5	astar	cactusADM	GemsFDTD	perlbench
mix6	cactusADM	GemsFDTD	gobmk	soplex
mix7	astar	cactusADM	leslie3d	sphinx3
mix8	bwaves	libquantum	perlbench	sphinx3
mix9	cactusADM	gobmk	milc	soplex
mix10	bzip2	gobmk	lbm	perlbench
mix11	astar	gobmk	milc	soplex
mix12	gobmk	leslie3d	libquantum	perlbench
mix13	bwaves	bzip2	gobmk	wrf
mix14	gobmk	lbm	leslie3d	milc
mix15	cactusADM	gobmk	milc	perlbench
mix16	bwaves	bzip2	gobmk	leslie3d
mix17	astar	bzip2	leslie3d	xalancbmk
mix18	gobmk	libquantum	wrf	xalancbmk
mix19	gobmk	lbm	milc	zeusmp
mix20	milc	perlbench	wrf	zeusmp

$$L_T = L_l + L_c$$

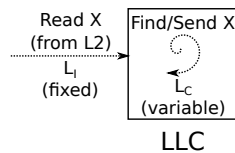


Fig. 6. Configuration of the LLC latency in ChampSim

## 6 EXPERIMENTAL RESULTS

This section presents performance results in a first time, and energy results in a second time. Both monore and multicore platforms are discussed.

### 6.1 Performance results

Performance results are presented as follows : firstly, we assess the impact of the LLC size in SRAM and STT-MRAM, by exploiting density to enlarge the cache capacity. Secondly, we report results when taking the Hawkeye cache replacement policy into account. Finally, we discuss this policy w.r.t. LRU. Except when it is explicitly mentioned, all results are normalized to the reference setup. For monore platforms, the reference is a 2MB SRAM LLC with LRU, i.e.,  $T_{sram\_lru}$ . For multicore platforms, it is a 4MB LLC with LRU, i.e.,  $S_{sram\_lru}$ .

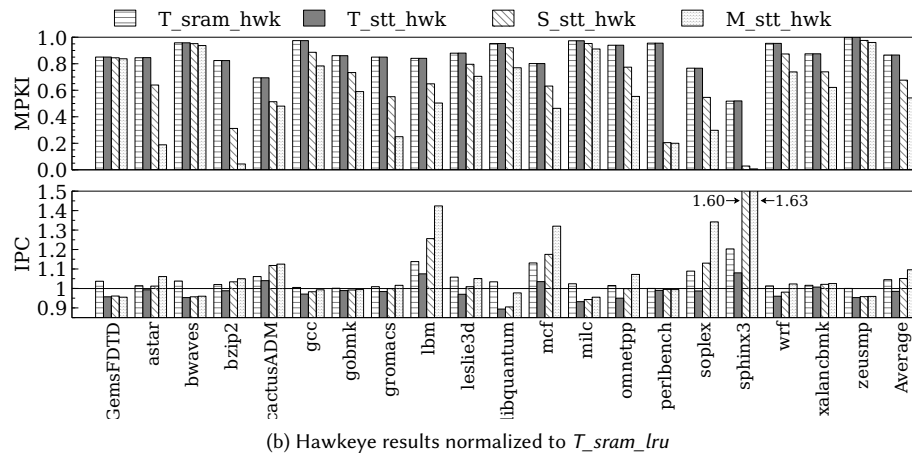
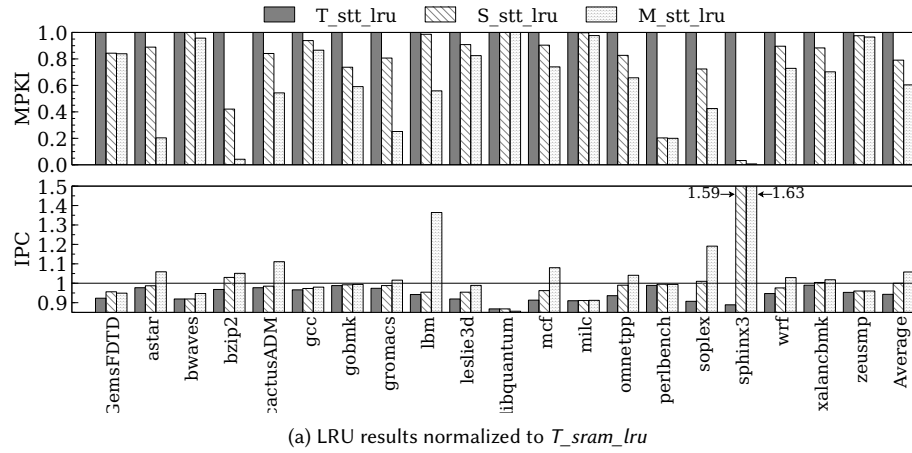
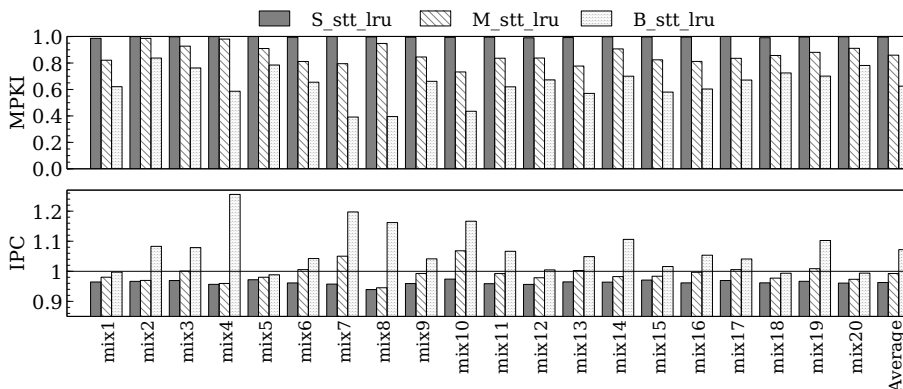


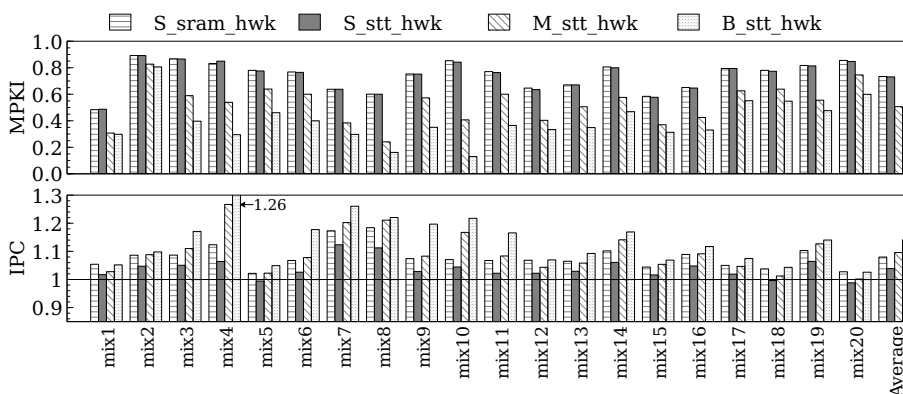
Fig. 7. MPKI (top) and IPC (bottom) for a moncore platform with LRU and Hawkeye replacement policies

**6.1.1 Impact of Cache Size and Technology.** Here, all configurations use the LRU replacement policy. The top of Figure 7a shows the MPKI improvement w.r.t. the reference configuration. We observe that the  $T_{stt\_lru}$  configuration does not influence the MPKI since the cache size remains unchanged. Conversely, a reduction of MPKI is clearly visible with  $S_{stt\_lru}$  and  $M_{stt\_lru}$  configurations. Some applications are not sensitive to cache size, like *bwaves*, *libquantum* or *milc*. Conversely, the *lbm* application is very sensitive to cache size from 8MB. For this application, the MPKI is decreased by a factor of 0.56 $\times$ . This indicates that a large part of the working set now fits into the LLC. Similar results are observed on Figure 8a for a multicore system. The MPKI is not changed with the default  $S_{stt\_lru}$  configuration, and is reduced with other configurations. Configuration  $B_{stt\_lru}$  reduces the MPKI up to 0.60 $\times$  with mixes 7 and 8.

The bottom part of Figure 7a shows the normalized IPC achieved by STT-MRAM configurations w.r.t the reference configuration. The  $T_{stt\_lru}$  configuration, i.e., a direct replacement of SRAM by STT-MRAM, is slower than the reference. This is due to the higher latency of STT-MRAM. The  $S_{stt\_lru}$  configuration gives on average the same



(a) LRU results normalized to  $S_{sram\_lru}$



(b) Hawkeye results normalized to  $S_{sram\_lru}$

Fig. 8. MPKI (top) and IPC (bottom) for a multicore platform with LRU and Hawkeye replacement policies

results than the reference, while the  $M_{stt\_lru}$  configuration outperforms the reference on average by  $1.06\times$ . With  $S_{stt\_lru}$  the IPC is degraded for sixteen applications, while it is only for nine applications with  $M_{stt\_lru}$ .

The performance for the *soplex* application is correlated to the MPKI. Indeed, there is a linear trend between MPKI reduction and IPC improvement. Conversely, the following applications, *gobmk*, *gromacs* and *perlbench* exhibit a significant MPKI reduction with no visible impact on performance. This is due to the very low amount of requests received by the LLC compared to the other applications. Hence, reducing this activity is not significant enough to improve the overall performance.

Results on multicore platforms (Figure 8a) follow the same trend as on a monore system. Configuration  $S_{stt\_lru}$  exhibits lower performance than the reference configuration  $S_{sram\_lru}$  due to the STT-MRAM latency. However, a bigger cache size is more efficient. The  $M_{stt\_lru}$  configuration provides a lower IPC for thirteen applications and  $B_{stt\_lru}$  for only four applications. As a result, the average gain on IPC with the largest configuration is  $1.07\times$ .

On average, increasing the LLC size shows that STT-MRAM could achieve the same or better performance as SRAM under area constraint for mono and multicore systems.

**6.1.2 Impact of Cache Replacement Policy.** Here, all configurations use the Hawkeye replacement policy. Performance results for a monore system are presented in Figure 7b. We observe the gains on the  $T\_sram\_hwk$  configuration, i.e., the Hawkeye reference. This configuration never degrades performances and achieves an average speedup of 1.05×. Larger STT-MRAM configurations,  $S\_stt\_hwk$  and  $M\_stt\_hwk$ , perform better than  $T\_sram\_hwk$  on average.

Thanks to the Hawkeye policy,  $T\_stt\_hwk$  and  $S\_stt\_hwk$  outperform the reference for *lbm* or *mcf*. This was not the case with LRU, as depicted in Figure 7a. Note that for a few applications such as *bwaves*, *GemsFDTD* or *zeusmp*, the  $T\_sram\_hwk$  configuration achieves a higher speedup than larger configurations with the same (or almost) MPKI. This shows that performance is still constrained by STT-MRAM latency, even with an enhanced replacement policy.

Nevertheless, Hawkeye improves performance where a larger cache only cannot. For example, all STT-MRAM configurations achieve the same IPC for the *milc* application with LRU, considering the LLC size. When Hawkeye is used, the performance is linearly increased with the cache size. As a matter of fact, Hawkeye can deal with some memory patterns not exploited by larger LLCs. The best configuration is  $M\_stt\_hwk$ , which achieves a performance improvement of 1.10× on average over the  $T\_sram\_lru$  baseline.

As with the LRU replacement policy, results for multicore systems on Figure 8b follow the same trend as on monore platforms. However, they are more valuable. The default configuration  $S\_stt\_hwk$  badly affects the IPC for only 3 applications (up to 1.2% for mix 20) while it is degraded for 15 applications on a monore platform. As a consequence, the average gain for the IPC with configurations  $M\_stt\_hwk$  and  $B\_stt\_hwk$  is respectively 1.09× and 1.14×. Configuration  $S\_stt\_hwk$  is the only STT-MRAM configuration that achieves lower results than  $S\_sram\_hwk$ , while its results are improved w.r.t. to  $S\_sram\_lru$ .

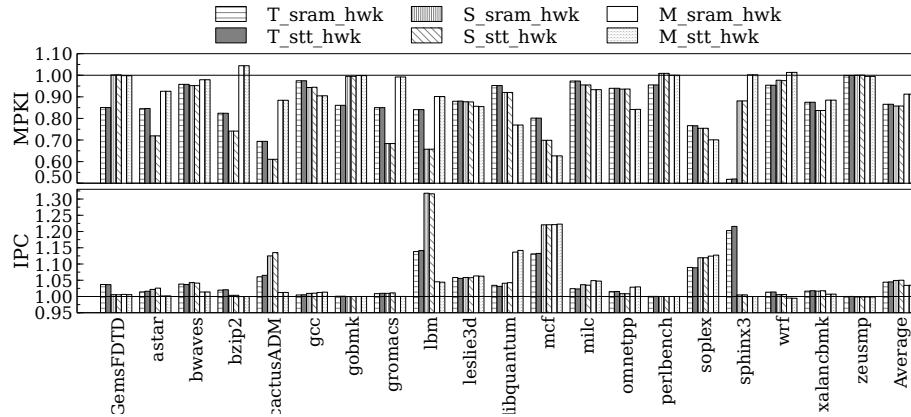


Fig. 9. Performance impact of Hawkeye normalized to LRU for a monore

**6.1.3 Hawkeye versus LRU.** In this section we focus only on results for a monore system to avoid redundancy. However, similar results are observed with a multicore platform.

Figure 9 shows the effect of the Hawkeye policy over LRU. Results are normalized for each configuration to its counterpart with LRU. For example,  $M\_stt\_hwk$  is normalized to  $M\_stt\_lru$ . For this experiment, we also run SRAM Working document

configuration that do not fit into area constraint to illustrate the effect of Hawkeye on SRAM and STT-MRAM for the same cache size. Both SRAM and STT-MRAM configurations follow the same trend regarding the MPKI reduction over LRU since the Hawkeye policy is not impacted by cache latency. Moreover, we use a single core platform where parallel events cannot occur. Hence, eviction decision remains identical for a given cache size, regardless of the cache size. However, the average gain obtained with Hawkeye is slightly better with STT-MRAM. The performance gap between SRAM and STT-MRAM is 3.3% and 3.1%, respectively with LRU and Hawkeye. Hence, reducing the amount of *write-fill* has higher impact on STT-MRAM where writes are penalizing.

Figure 9 shows that the 8MB configuration is not as efficient as the 4MB configuration in terms of performance improvement. The average gain for the IPC for  $M\_sram\_hwk$  and  $M\_stt\_hwk$  is lower than  $S\_sram\_hwk$  and  $S\_stt\_hwk$ . This suggests an issue that can be due to either a larger LLC, or the Hawkeye policy, or both. Even if the overall performance improvement reported in Figure 7b shows that the 8MB configuration is faster, we note that there may be a limit to the performance improvement provided by the Hawkeye policy. This behavior is visible with *bzip2*, *wrf* and *sphinx3*. In Figure 7a, results show that the MPKI is reduced for  $S\_stt\_lru$  and  $M\_stt\_lru$ . Hence, increasing the cache size is efficient. Similarly, in Figure 7b, the MPKI is also reduced for the same configurations while replacing LRU by Hawkeye. However, the gains observed in Figure 9 show that Hawkeye increases the MPKI compared to LRU for a 8MB LLC. The reason is that Hawkeye made inadequate eviction decisions. Indeed, the Hawkeye predictor exploits cache accesses to identify the instructions that generate cache misses. Since a large cache size reduces the number of cache misses, it becomes more difficult for the predictor to learn accurately from a small set of miss events. Note that the performance for  $M\_stt\_hwk$  is still better than other configurations despite these inaccurate decisions.

## 6.2 Energy results

In this section, we present the energy consumption and energy-efficiency results with LRU and Hawkeye replacement policies. We first describe our results for a monore platform, and secondly for a multicore platform. For the rest of the paper, the energy-efficiency is characterized as the Energy-Delay Product (EDP).

**6.2.1 Entire system perspective.** Figure 10a depicts results for the energy consumption (top) and the EDP (bottom) for a monore system with LRU. On average, configurations  $T\_stt\_lru$ ,  $S\_stt\_lru$  and  $M\_stt\_lru$  reduce the energy consumption respectively by a factor 0.89 $\times$ , 0.86 $\times$  and 0.83 $\times$ . The application *libquantum* is the only application where the energy consumption is increased. This is explained by the higher execution time due to longer STT-MRAM latency (Figure 7a). The Energy-Delay Product is correlated to the energy consumption. On average, the gain w.r.t. the SRAM reference is 0.95 $\times$ , 0.86 $\times$  and 0.79 $\times$  respectively for configurations  $T\_stt\_lru$ ,  $S\_stt\_lru$  and  $M\_stt\_lru$ . However, some applications like *bwaves*, *libquantum* or *milc* badly affect the EDP compared to the SRAM reference  $T\_sram\_lru$ . These applications suffer from a too important slowdown in terms of execution time, due to their insensibility to the LLC size (Figure 7a).

Results with the Hawkeye replacement policies on Figure 10b show that the SRAM configuration  $T\_sram\_hwk$  provides a small gain of 0.95 $\times$  in terms of energy consumption. The low power feature of the STT-MRAM technology increase this gain up to 0.85 $\times$ , 0.81 $\times$  and 0.80 $\times$  respectively for configurations  $T\_stt\_hwk$ ,  $S\_stt\_hwk$  and  $M\_stt\_hwk$ . With the Hawkeye replacement policy, gains are more noticeable and no degradation can be observed as with the LRU. The EDP is also improved, and only *bwaves* and *libquantum* applications exhibit a higher EDP w.r.t.  $T\_sram\_lru$ . The best average EDP is provided by configuration  $M\_stt\_hwk$ .

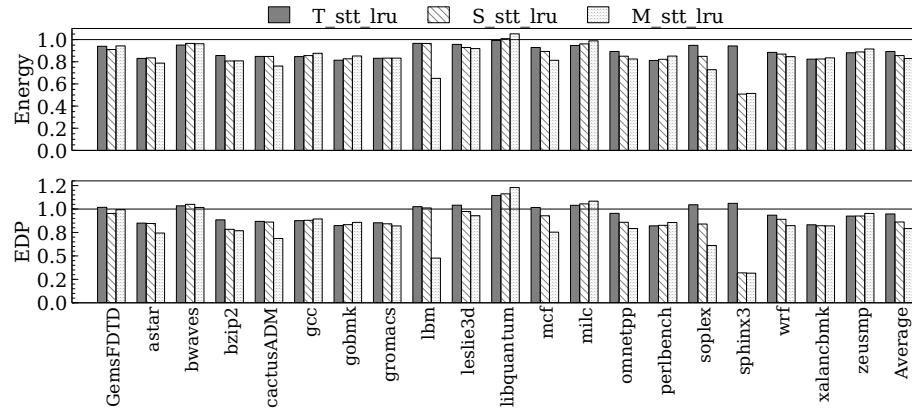
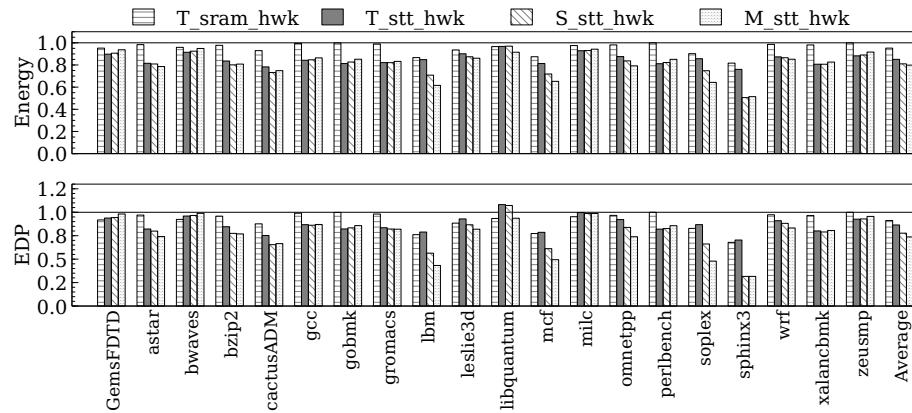
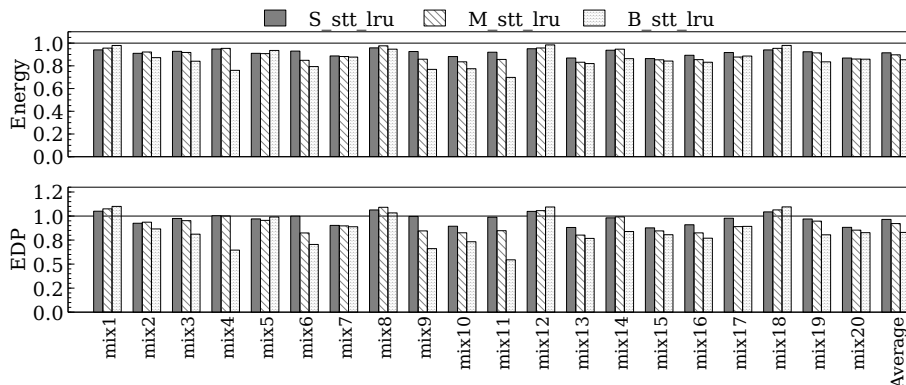
(a) LRU results normalized to  $T_{sram\_lru}$ (b) Hawkeye results normalized to  $T_{sram\_lru}$ 

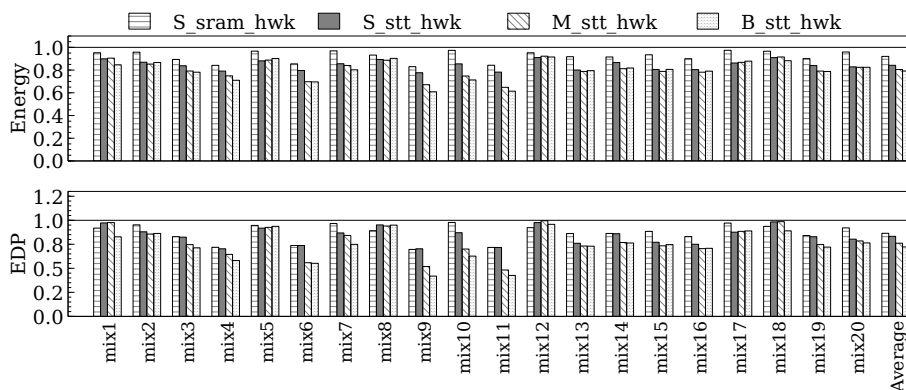
Fig. 10. Energy consumption (top) and EDP (bottom) for a monocoore platform with LRU and Hawkeye replacement policies

Thanks to the low-power feature of the STT-MRAM, results for multicore platform show a decrease of the energy consumption for all considered mixes. However, one can observe on Figure 11a that for mixes 1, 12 and 18, the energy consumption increases as the cache size is scaled. This is due to a higher execution time related to the STT-MRAM latency that increases with cache size. On average, we observe an energy consumption improvement of  $0.91\times$ ,  $0.90\times$  and  $0.85\times$  respectively for configurations  $T_{stt\_lru}$ ,  $S_{stt\_lru}$  and  $M_{stt\_lru}$ . Regarding the EDP, we observe a counter-performance for mix 1, 12, 18 and 8. For the first three, this is due to their higher execution time previously mentioned. Performance of mix 8 on Figure 8b show an improvement, up to  $1.20\times$  with  $B_{stt\_lru}$  configuration, while the energy consumption reduction with this cache configuration is slight and similar to configuration  $T_{stt\_lru}$ . This is due to the *sphinx3* application in the mix, that achieves an IPC improvement of  $1.50\times$ , while others applications suffers from IPC reduction of  $0.98\times$ ,  $0.91\times$  and  $0.99\times$ . The geometric mean shows an average improvement while the global execution time of mix 8 is increased by  $1.09\times$ . This explain the low improvement in terms of EDP. Results with the Hawkeye replacement policy are presented by Figure 11b. They follow a similar trend as with LRU, with more significant reductions on the Working document

energy consumption. The improvement is gradual as the cache size increases. The EDP results are correlated to this observation, and the best average EDP improvement is achieved by configuration  $B\_stt\_hwk$  by  $0.79\times$ .



(a) Energy consumption and EDP for a multicore platform with LRU



(b) Energy consumption and EDP for a multicore platform with Hawkeye

Fig. 11. Energy consumption and EDP for a multicore platform with LRU and Hawkeye replacement policies

**6.2.2 Last-Level Cache perspective.** In the previous section, we present the energy consumption results for the entire system. Here, we rather focus on the Last-Level Cache and the impact of the Hawkeye replacement policy. For the sake of simplicity, this analysis is conducted on a monore platform, but results for multicore platform are similar.

Figure 12 illustrates the impact of Hawkeye on the energy consumption. For each cache application, the energy consumption with Hawkeye is normalized to its counterpart with LRU. On average, the effect is positive and the LLC consumes less energy with Hawkeye. However, results show the opposite for few applications, like *wrf* or *GemsFDTD*. With these applications, the energy consumption is always greater with Hawkeye than with LRU. This situation is due to changes on transactions on the LLC, as discussed in Section 3.3.

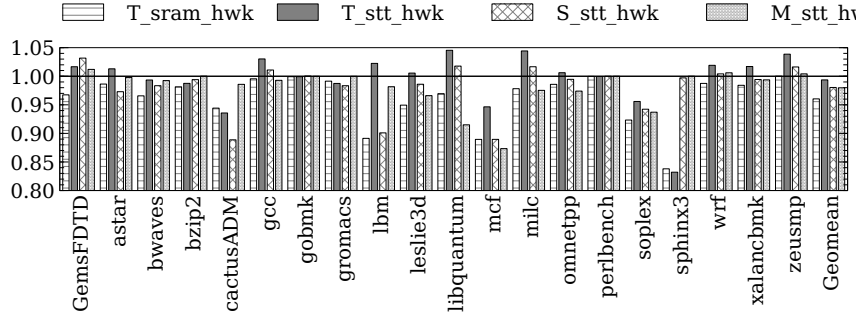


Fig. 12. Energy impact of the Hawkeye replacement policy on a monore platform. For each configuration with Hawkeye, result is normalized to its counterpart with LRU.

Table 6. Evolution of the number of transactions received by the LLC with the Hawkeye replacement policy

Metric	Read hit	Read miss	Write-back hit	Write-back miss
<i>GemsFDTD</i>	0.98×	1.0×	0.44×	2400×
<i>libquantum</i>	2.10 <sup>6</sup>	0.92×	0.17×	7.10 <sup>6</sup> ×
<i>milc</i>	16×	0.96×	0.26×	6.10 <sup>5</sup> ×
<i>wrf</i>	1.08×	0.98×	0.83×	450×

Table 6 gives the total amount of *read hit*, *read miss*, *write-back hit* and *write-back miss* for four applications with a 4MB cache: *GemsFDTD*, *libquantum*, *milc* and *wrf*. On one hand, this illustrates the positive effect of Hawkeye. Except for *GemsFDTD*, the total number of *read hit* is increased, while the number of *read miss* is identical or decreased. Considering Formula 1, variable  $P_r^h$  is increased and the energy cost due to misses is decreased. On the other hand, we can observe the negative impact of the Hawkeye strategy. The number of *write-back hit* is largely reduced, from 0.83× and up to 0.17×, while the number of *write-back miss* is drastically increased, from 450× and up to 7.10<sup>6</sup>×. Considering Formula 2, one can observe that when  $P_w^h$  is decreased, then additional miss costs are added and writing is more expensive.

Upon a certain threshold, the energy gains obtained by decreasing the number of *read miss* become less important than additional costs due to an increasing number of *write-back miss*. Hence, the global energy consumption of the LLC is increased.

## 7 CONCLUSION

This paper evaluates the impact of a *state-of-the-art* replacement policy used along with STT-MRAM technology on monore and multicore architectures. The high density feature of the STT-MRAM is used to increase the cache size, while the replacement policy is used to improve the overall performance. Moreover, the low-power aspect of the STT-MRAM allows a designer to decrease the energy consumption.

We analyze the two different types of write that exists in the memory hierarchy and showed that they are more important than *write-back* for performance improvement since they are on the *critical path* to main memory access. Thus, we applied the Hawkeye replacement policy which is designed for reducing cache read misses. However, pre-simulation

analysis and experimental results suggest that this policy could have a negative impact on the energy consumption of the LLC for a certain class of applications.

We showed that using such policy with STT-MRAM is more beneficial than with SRAM. Indeed, the read/write latency asymmetry of this technology allows a higher gap of improvement in terms of performance than with SRAM. However, with a large cache that drastically reduces the number of misses, the small amount of accesses makes the training of the Hawkeye predictor longer. Thus, it leads to inadequate eviction decisions. The evaluation results showed that performance can be improved up to 10% and 14% respectively for monocore and multicore platform. This gain, combined with the drastic static energy reduction enabled by STT-MRAM, leads to increased energy-efficiency up to 26.3%× and 27.7% for monocore and multicore systems.

## ACKNOWLEDGEMENTS

This work has been funded by the French ANR agency under the grant ANR-15-CE25-0007-01, within the framework of the CONTINUUM project.

## REFERENCES

- [1] [n.d.]. The ChampSim simulator. <https://github.com/ChampSim>.
- [2] [n.d.]. DDR3-Micron MT41K512M8DA-125 datasheet. <https://bit.ly/2x1HIG5>, last accessed Sept. 2018.
- [3] [n.d.]. ISCA 2017 Cache Replacement Championship. <http://crc2.ece.tamu.edu>.
- [4] 2015. International Technology Roadmap for Semiconductors (ITRS).
- [5] Laszlo A. Belady. 1966. A Study of Replacement Algorithms for a Virtual-Storage Computer. *IBM Systems journal* 5, 2 (1966), 78–101.
- [6] Nathan Binkert, Bradford Beckmann, Gabriel Black, Steven K. Reinhardt, Ali Saidi, Arkaprava Basu, Joel Hestness, Derek R. Hower, Tushar Krishna, Somayeh Sardashti, Rathijit Sen, Korey Sewell, Muhammad Shoaib, Nilay Vaish, Mark D. Hill, and David A. Wood. 2011. The Gem5 Simulator. *SIGARCH Comput. Archit. News* 39, 2 (Aug. 2011), 1–7. <https://doi.org/10.1145/2024716.2024718>
- [7] Rabab Bouziane, Erven Rohou, and Abdoulaye Gamatié. 2017. How Could Compile-Time Program Analysis help Leveraging Emerging NVM Features?. In *EDIS: Embedded and Distributed Systems*. Oran, Algeria, 1–6. <https://doi.org/10.1109/EDIS.2017.8284031>
- [8] Rabab Bouziane, Erven Rohou, and Abdoulaye Gamatié. 2018. Compile-Time Silent-Store Elimination for Energy Efficiency: an Analytic Evaluation for Non-Volatile Cache Memory. In *Procs of the Rapido'18 Workshop on Rapid Simulation and Performance Evaluation: Methods and Tools*. ACM, 5.
- [9] Rabab Bouziane, Erven Rohou, and Abdoulaye Gamatié. 2018. Energy-Efficient Memory Mappings Based on Partial WCET Analysis and Multi-Retention Time STT-RAM. In *Proceedings of the 26th International Conference on Real-Time Networks and Systems (Chasseneuil-du-Poitou, France) (RTNS '18)*. Association for Computing Machinery, New York, NY, USA, 148–158. <https://doi.org/10.1145/3273905.3273908>
- [10] Doug Burger and Todd M. Austin. 1997. The SimpleScalar Tool Set, Version 2.0. *SIGARCH Comput. Archit. News* 25, 3 (June 1997), 13–25. <https://doi.org/10.1145/268806.268810>
- [11] Anastasiia Butko, Abdoulaye Gamatié, Gilles Sassatelli, Lionel Torres, and Michel Robert. 2015. Design Exploration for next Generation High-Performance Manycore On-chip Systems: Application to big.LITTLE Architectures. In *ISVLSI: International Symposium on Very Large Scale Integration*. IEEE, Montpellier, France, 551–556. <https://doi.org/10.1109/ISVLSI.2015.28>
- [12] Anastasiia Butko, Rafael Garibotti, Luciano Ost, Vianney Lapotre, Abdoulaye Gamatié, Gilles Sassatelli, and Chris Adeniyi-Jones. 2015. A trace-driven approach for fast and accurate simulation of manycore architectures. In *The 20th Asia and South Pacific Design Automation Conference, ASP-DAC 2015, Chiba, Japan, January 19-22, 2015*. IEEE, 707–712. <https://doi.org/10.1109/ASP-DAC.2015.7059093>
- [13] Thibaud Delobelle, Pierre-Yves Péneau, Abdoulaye Gamatié, Florent Bruguier, Sophiane Senni, Gilles Sassatelli, and Lionel Torres. 2017. MAGPIE: System-level Evaluation of Manycore Systems with Emerging Memory Technologies. In *EMS: Emerging Memory Solutions*. Lausanne, Switzerland. <https://hal-lirmm.ccsd.cnrs.fr/lirmm-01467328>
- [14] Thibaud Delobelle, Pierre-Yves Péneau, Sophiane Senni, Florent Bruguier, Abdoulaye Gamatié, Gilles Sassatelli, and Lionel Torres. 2016. Flot automatique d'évaluation pour l'exploration d'architectures à base de mémoires non volatiles. In *CompAS: Conférence en Parallélisme, Architecture et Système*. Lorient, France. <https://hal-lirmm.ccsd.cnrs.fr/lirmm-01345975>
- [15] Xiangyu Dong, Cong Xu, Yuan Xie, and Norman P Jouppi. 2012. NVSim: A Circuit-Level Performance, Energy, and Area Model for Emerging Nonvolatile Memory. *IEEE Trans. on Computer-Aided Design of Integ. Circ. and Sys.* 31, 7 (2012), 994–1007.
- [16] J Gecsei, DR Slutz, and IL Traiger. 1970. Evaluation Techniques for Storage Hierarchies. *IBM Systems journal* 9, 2 (1970), 78–117.
- [17] John L Henning. 2006. SPEC CPU2006 benchmark descriptions. *ACM SIGARCH Computer Architecture News* 34, 4 (2006), 1–17.
- [18] Akanksha Jain and Calvin Lin. 2016. Back to the Future: Leveraging Belady's Algorithm for Improved Cache Replacement. In *Computer Architecture (ISCA), 2016 ACM/IEEE 43rd Annual International Symposium on*. IEEE, 78–89.

- [19] Aamer Jaleel, Kevin B Theobald, Simon C Steely Jr, and Joel Emer. 2010. High Performance Cache Replacement Using Re-Reference Interval Prediction (RRIP). In *ACM SIGARCH Computer Architecture News*, Vol. 38. ACM, 60–71.
- [20] Namhyung Kim, Junwhan Ahn, Woong Seo, and Kiyoung Choi. 2015. Energy-efficient exclusive last-level hybrid caches consisting of SRAM and STT-RAM. In *2015 IFIP/IEEE International Conference on Very Large Scale Integration (VLSI-SoC)*. 183–188. <https://doi.org/10.1109/VLSI-SoC.2015.7314413>
- [21] Jing Li, Patrick Ndai, Ashish Goel, Sayeef Salahuddin, and Kaushik Roy. 2010. Design Paradigm for Robust Spin-Torque Transfer Magnetic RAM (STT MRAM) from Circuit/Architecture Perspective. *IEEE Tran. on Very Large Scale Integration Systems* 18, 12 (2010), 1710–1723.
- [22] Qingan Li, Liang Shi, Jianhua Li, Chun Jason Xue, and Yanxiang He. 2012. Code Motion for Migration Minimization in STT-RAM Based Hybrid Cache. In *VLSI (ISVLSI), 2012 IEEE Computer Society Annual Symposium on*. IEEE, 410–415.
- [23] Chen Liu, Yuanqing Cheng, Ying Wang, Youguang Zhang, and Weisheng Zhao. 2018. NEAR: A Novel Energy Aware Replacement Policy for STT-MRAM LLCs. In *IEEE Int'l Symp. on Circuits and Systems (ISCAS)*. 1–5.
- [24] Liu Liu, Ping Chi, Shuangchen Li, Yuanqing Cheng, and Yuan Xie. 2017. Building Energy-Efficient Multi-Level Cell STT-RAM Caches With Data Compression. In *Asia and South Pacific Design Automation Conf*. 751–756.
- [25] Zihao Liu, Mengjie Mao, Tao Liu, Xue Wang, Wujie Wen, Yiran Chen, Hai Li, Danghui Wang, Yukui Pei, and Ning Ge. 2018. TriZone: A Design of MLC STT-RAM Cache for Combined Performance, Energy, and Reliability Optimizations. *IEEE Transactions on Computer-Aided Design of Integrated Circuits and Systems* 37, 10 (Oct. 2018), 1985–1998.
- [26] Jing-Yuan Luo, Hsiang-Yun Cheng, Ing-Chao Lin, and Da-Wei Chang. 2019. TAP: Reducing the Energy of Asymmetric Hybrid Last-Level Cache via Thrashing Aware Placement and Migration. *IEEE Trans. Comput.* 68, 12 (2019), 1704–1719. <https://doi.org/10.1109/TC.2019.2917208>
- [27] Deepak M Mathew, Éder F Zulian, Subash Kannoth, Matthias Jung, Christian Weis, and Norbert Wehn. 2017. A Bank-Wise DRAM Power Model for System Simulations. In *Proceedings of the 9th Workshop on Rapid Simulation and Performance Evaluation: Methods and Tools*. ACM, 5.
- [28] Sparsh Mittal. 2014. A Survey of Architectural Techniques for Improving Cache Power Efficiency. *Sustainable Computing: Informatics and Systems* 4, 1 (2014), 33–43.
- [29] Sparsh Mittal. 2017. A Survey of Soft-Error Mitigation Techniques for Non-Volatile Memories. *Computers* 6, 1 (2017), 8.
- [30] Sparsh Mittal and Jeffrey S Vetter. 2015. AYUSH: A Technique for Extending Lifetime of SRAM-NVM Hybrid Caches. *Computer Architecture Letters* 14, 2 (2015), 115–118.
- [31] Alejandro Nocua, Florent Bruguier, Gilles Sassatelli, and Abdoulaye Gamatié. 2017. ElasticSimMATE: A fast and accurate gem5 trace-driven simulator for multicore systems. In *12th International Symposium on Reconfigurable Communication-centric Systems-on-Chip, ReCoSoC 2017, Madrid, Spain, July 12-14, 2017*. IEEE, 1–8. <https://doi.org/10.1109/ReCoSoC.2017.8016146>
- [32] Pierre-Yves Péneau, David Novo, Florent Bruguier, Lionel Torres, Gilles Sassatelli, and Abdoulaye Gamatié. 2018. Improving the Performance of STT-MRAM LLC Through Enhanced Cache Replacement Policy. In *Architecture of Computing Systems - ARCS 2018 - 31st International Conference, Braunschweig, Germany, April 9-12, 2018, Proceedings (Lecture Notes in Computer Science, Vol. 10793)*, Mladen Berekovic, Rainer Buchty, Heiko Hamann, Dirk Koch, and Thilo Pionteck (Eds.). Springer, 168–180. [https://doi.org/10.1007/978-3-319-77610-1\\_13](https://doi.org/10.1007/978-3-319-77610-1_13)
- [33] Pierre-Yves Péneau, Rabab Bouziane, Abdoulaye Gamatié, Erven Rohou, Florent Bruguier, Gilles Sassatelli, Lionel Torres, and Sophiane Senni. 2016. Loop Optimization in Presence of STT-MRAM Caches: A Study of Performance-Energy Tradeoffs. In *Power and Timing Modeling, Optimization and Simulation (PATMOS), 2016 26th International Workshop on*. IEEE, 162–169.
- [34] Pierre-Yves Péneau, Florent Bruguier, David Novo, Gilles Sassatelli, and Abdoulaye Gamatié. 2020. *Towards a Flexible and Comprehensive Evaluation Approach for Addressing NVM Integration in Cache Hierarchy*. Technical Report. LIRMM, CNRS, Univ. Montpellier.
- [35] Pierre-Yves Péneau, David Novo, Florent Bruguier, Gilles Sassatelli, and Abdoulaye Gamatié. 2017. Performance and Energy Assessment of Last-Level Cache Replacement Policies. In *Embedded & Distributed Systems (EDiS), 2017 First International Conference on*. IEEE, 1–6.
- [36] Fernando Magno Quintão Pereira, Guilherme Vieira Leobas, and Abdoulaye Gamatié. 2018. Static Prediction of Silent Stores. *ACM Trans. Archit. Code Optim.* 15, 4, Article 44 (Nov. 2018), 26 pages. <https://doi.org/10.1145/3280848>
- [37] Bhukya Krishna Priya, Sampath Kumar, Shameedha Begum, and N. Ramasubramaniam. 2018. Enhancing the lifetime of STT-RAM with MRU replacement algorithm. In *2018 4th International Conference on Recent Advances in Information Technology (RAIT)*. 1–6. <https://doi.org/10.1109/RAIT.2018.8388985>
- [38] Moinuddin K Qureshi, Aamer Jaleel, Yale N Patt, Simon C Steely, and Joel Emer. 2007. Adaptive Insertion Policies for High Performance Caching. In *ACM SIGARCH Computer Architecture News*, Vol. 35. ACM, 381–391.
- [39] Sophiane Senni, Raphael Martins Brum, Lionel Torres, Gilles Sassatelli, Abdoulaye Gamatié, and Bruno Mussard. 2015. Potential applications based on NVM emerging technologies. In *Proceedings of the 2015 Design, Automation & Test in Europe Conference & Exhibition, DATE 2015, Grenoble, France, March 9-13, 2015*, Wolfgang Nebel and David Atienza (Eds.). ACM, 1012–1017. <http://dl.acm.org/citation.cfm?id=2757049>
- [40] Sophiane Senni, Thibaud Delobelle, Odilia Coi, Pierre-Yves Péneau, Lionel Torres, Abdoulaye Gamatié, Pascal Benoit, and Gilles Sassatelli. 2017. Embedded Systems to High Performance Computing Using STT-MRAM. In *2017 Design, Automation & Test in Europe Conference & Exhibition (DATE)*. IEEE, 536–541.
- [41] Sophiane Senni, Lionel Torres, Gilles Sassatelli, Abdoulaye Gamatié, and Bruno Mussard. 2016. Exploring MRAM Technologies for Energy Efficient Systems-On-Chip. *IEEE Journal on Emerging and Selected Topics in Circuits and Systems* 6, 3 (2016), 279–292. <https://doi.org/10.1109/JETCAS.2016.2547680>
- [42] Clinton W Smullen, Vidyabhushan Mohan, Anurag Nigam, Sudhanva Gurumurthi, and Mircea R Stan. 2011. Relaxing Non-Volatility for Fast and Energy-Efficient STT-RAM Caches. In *High Performance Computer Architecture (HPCA), 2011 IEEE 17th International Symposium on*. IEEE, 50–61.

- [43] Guangyu Sun, Xiangyu Dong, Yuan Xie, Jian Li, and Yiran Chen. 2009. A Novel Architecture of the 3D Stacked MRAM L2 Cache for CMPs. In *High Performance Computer Architecture, 2009. HPCA 2009. IEEE 15th International Symposium on*. IEEE, 239–249.
- [44] Mohammad Taghi Teimoori, Muhammad Abdullah Hanif, Alireza Ejlali, and Muhammad Shafique. 2018. AdAM: Adaptive approximation management for the non-volatile memory hierarchies. In *2018 Design, Automation Test in Europe Conference Exhibition (DATE)*. 785–790. <https://doi.org/10.23919/DATE.2018.8342113>
- [45] K Ananda Vardhan and YN Srikant. 2014. Exploiting Critical Data Regions to Reduce Data Cache Energy Consumption. In *Proceedings of the 17th International Workshop on Software and Compilers for Embedded Systems*. ACM, 69–78.
- [46] Jeffrey S Vetter and Sparsh Mittal. 2015. Opportunities for Nonvolatile Memory Systems in Extreme-Scale High-Performance Computing. *Computing in Science & Engineering* 17, 2 (2015), 73–82.
- [47] Jianxing Wang, Yenni Tim, Weng-Fai Wong, Zhong-Liang Ong, Zhenyu Sun, and Hai Li. 2014. A Coherent Hybrid SRAM and STT-RAM L1 Cache Architecture for Shared Memory Multicores. In *Asia and South Pacific Design Automation Conference (ASP-DAC)*. IEEE, 610–615.
- [48] Xiaoxia Wu, Jian Li, Lixin Zhang, Evan Speight, Ram Rajamony, and Yuan Xie. 2009. Hybrid Cache Architecture with Disparate Memory Technologies. In *ACM SIGARCH computer architecture news*, Vol. 37. ACM, 34–45.
- [49] Sadegh Yazdanshenas, Marzieh Ranjbar Pirbasti, Mahdi Fazeli, and Ahmad Patooghy. 2014. Coding Last Level STT-RAM Cache for High Endurance and Low Power. *IEEE Comp. Arch. Letters* 13, 2 (2014), 73–76.
- [50] Ping Zhou, Bo Zhao, Jun Yang, and Youtao Zhang. 2009. Energy Eeduction for STT-RAM Using Early Write Termination. In *Computer-Aided Design-Digest of Technical Papers, 2009. ICCAD 2009. IEEE/ACM International Conference on*. IEEE, 264–268.